Published in Cretaceous Research 29, issues 5-6, 830-847, 2008
which should be used for any reference to this work

Platform-induced clay-mineral fractionation along a northern Tethyan basin-platform transect: implications for the interpretation of Early Cretaceous climate change (Late Hauterivian-Early Aptian)

Alexis Godet [a,b,*], Stéphane Bodin [a,c], Thierry Adatte [a,d], Karl B. Föllmi

[a] *Institute of Geology, University of Neuchâtel, rue Emile Argand 11, CP 158 2009 Neuchâtel, Switzerland*
[b] *Neftex Petroleum Consultants Ltd., 115BD Milton Park, Abingdon, Oxfordshire OX14 4SA, United Kingdom*
[c] *North Africa Research Group, School of Earth, Atmospheric and Environmental Science, University of Manchester, Williamson Building, Oxford Road, Manchester M13 9PL, United Kingdom*
[d] *Institut de Géologie et Paléontologie, Université de Lausanne, Anthropôle, CH 1015 Lausanne, Switzerland*

A B S T R A C T

High-resolution clay-mineral analyses were performed on upper Hauterivian to lower Aptian sediments along a platform-to-basin transect through the northern Tethyan margin from the Neuchâtel area (Switzerland), to the Vocontian Trough (France) in order to investigate links between climate change, carbonate platform evolution, and fractionation patterns in clay minerals during their transport.

During the Hauterivian, the northern Tethyan carbonate platform developed in a heterozoan mode, and the associated ramp-like topography facilitated the export of detrital material into the adjacent basin, where clay-mineral assemblages are dominated by smectite and kaolinite is almost absent, thereby suggesting dry-seasonal conditions. During the Late Hauterivian *Balearites balearis* ammonite zone, a change to a more humid climate is documented by the appearance of kaolinite, which reaches up to 30% of the clay fraction in sediments in the Vocontian Trough. This prominent change just preceded the Faraoni Oceanic Anoxic Event and the onset of the demise of the Helvetic Carbonate Platform, which lasted to the late early Barremian.

From the Late Barremian onwards, the renewed growth of the northern Tethyan carbonate platform in a photozoan mode and the associated development of a marginally confined platform topography fractionated the clay-mineral assemblages exported into hemipelagic settings: kaolinite particles were preferentially retained in proximal, platform settings, due to their size and their relatively high specific weight. In the inner platform environment preserved in the Swiss Jura, an average of 32% of kaolinite in the clay fraction is observed during the latest Barremian–earliest Aptian, whereas clay-mineral assemblages of coeval sediments from deeper depositional settings are dominated by smectite and show only minor amounts of kaolinite.

This signifies that besides palaeoclimate conditions, the morphology and ecology of the carbonate platform had a significant effect on the distribution and composition of clay assemblages during the Late Hauterivian–Early Aptian along the northern Tethyan margin.

Kaolinite Climate change, Early Cretaceous, Carbonate platform, Jura Mountains, Vocontian Trough

1. Introduction

The Early Cretaceous climate was sustained by generally elevated atmospheric pCO_2 (e.g., Berner and Kothavala, 2001), implying reinforced greenhouse conditions, which influenced the water cycle, the intensity of rainfall, and the biogeochemical weathering of continental rocks (e.g., Weissert, 1989; Weissert et al., 1998; Larson and Erba, 1999). The latter may have affected marine biological communities by regulating the input of nutrients in the ocean; episodes of enhanced nutrients transfer to the ocean may have led to increased marine productivity rates and the subsequent generation and preservation of organic-rich sediments under partly anoxic conditions.

An example of such an episode is documented by the Late Hauterivian Faraoni Level, which was first described in the Umbria-Marche basin of Italy (Cecca et al., 1995), and subsequently recovered in sections from other regions of the central and western Tethys (Baudin, 2005). The Faraoni Level displays features similar to other Oceanic Anoxic Events (OAE's; e.g., Schlanger and Jenkyns, 1976; Scholle and Arthur, 1980) such as the presence of finely

* Corresponding author.
E-mail address: alexis.godet@unine.ch (A. Godet).

laminated black-shale facies with TOC values of more than 10% in Italian sections. However, unlike other Cretaceous OAE's, the Faraoni Level is not associated with a carbon isotope excursion and only marked by an increase of 0.15‰ in sediments from the western Switzerland and southeastern France (Baudin et al., 1999; Godet et al., 2006); by comparison, the OAE1a (Early Aptian) is associated to a negative spike (amplitude of ca. −1.5‰) followed by a positive excursion (amplitude of ca. +2‰; e.g., Föllmi et al., 2006). This is explained by a buffering effect on the marine $\delta^{13}C$ record, through accelerated water cycle and increased delivery of Dissolved Inorganic Carbon (DIC) to the ocean under more humid climate conditions (e.g., Bartley and Kah, 2004; Godet et al., 2006).

Climate change during the Early Cretaceous has been deduced from the temporal evolution of clay-mineral assemblages (e.g., Ruffell and Batten, 1990; Ruffell et al., 2002). Clay minerals are valid indicators of the intensity of geochemical weathering processes on the continent, because such processes are influenced by climate (humidity, average temperature, seasonality; e.g., Chamley, 1981; Ruffell et al., 2002). Geomorphology is in turn an expression of tectonic and climatic processes. Investigations of clay minerals in Barremian sediments of Western Europe (Spain, England, France, and Germany) have led to the interpretation of a relatively stable dry climate, which was probably interrupted by short-term changes from arid to semi-arid conditions, as is indicated by the occurrence of traces of kaolinite (Ruffell and Batten, 1990). Upper Jurassic–Lower Cretaceous sediments from the Jura Mountains contain relatively high amounts of kaolinite (up to 30%), except in Hauterivian sediments where smectite represents up to 50% of the clay fraction, which suggests seasonally contrasted conditions for this stage (Persoz, 1982; Adatte and Rumley, 1989).

Here we show the results of our analysis of clay-mineral assemblages from a selection of sections of Hauterivian and Barremian age along a transect through the northern Tethyan margin, which ranges from the hemipelagic Vocontian Trough to the platform environment preserved in the Jura Mountains. We use this data set to reconstruct the evolution of climate during the Hauterivian and Barremian along the northern Tethyan margin. Then, we propose to deduct the potential effect of this type of environmental change on the continental hydrological cycle and intensity in chemical weathering processes; the related transfer of nutrients and DIC into the ocean will be taken into consideration, as well as the corresponding impact on the marine environment and marine carbon isotope system. We also consider the impact of different carbonate platform morphologies associated with photozoan and heterozoan production modes on the spatial distribution of clay minerals, especially kaolinite.

2. Geological setting and location of the studied sections

The sections of La Charce, Vergons, Angles (stratotype of the Barremian stage), and Combe-Lambert are located in the region of the Alpes de Haute Provence, southeastern France (Figs. 1–3). They represent a hemipelagic environment typical for the Vocontian Trough, and the abundance of ammonites allows for excellent time-calibration (e.g., Bulot et al., 1992; Delanoy, 1997; Vermeulen, 2002). During the Early Cretaceous, the Vocontian Trough constituted an epicontinental basin, which was surrounded by carbonate platforms such as the Bas-Dauphiné platform and which was connected to the Ligurian Tethys (e.g., Baudin et al., 1999).

Located in France, approximately 20 km southeastward from Geneva (Fig. 1), the section of Cluses (Fig. 4) belongs to the Bornes Massif, which constitutes the northeastern part of the French Subalpine Chains (e.g., Trabold, 1996). In the absence of ammonites in these facies, which is similar to that of the Helvetic ramp, the dating of the Cluses section is mainly based on orbitolinids and echinoids (Trabold, 1996; Wermeille, 1996).

Finally, the Eclépens section is located between Neuchâtel and Lausanne (Switzerland), and belongs to the Western Swiss Jura (Figs. 1 and 5). This region hosts the historical succession of the Hauterivian stage, first described by de Montmollin (1835), which is composed, from the base to the top, by the "Marne à Astiera," the "Marne Bleue d'Hauterive," and the "Pierre Jaune de Neuchâtel" (PJN). Whereas the age of these formations is well-constrained by ammonite biostratigraphy, the overlying "Urgonien Jaune" (UJ) and "Urgonien Blanc" (UB) are lacking ammonites; based on recent nannofossils finding near the base of the UJ, these formations are attributed to the Late Barremian–Earliest Aptian (Godet et al., 2005). The study of Blanc-Aletru (1995) on the upper part of the section (UJ and UB) are complementary to the results of this work.

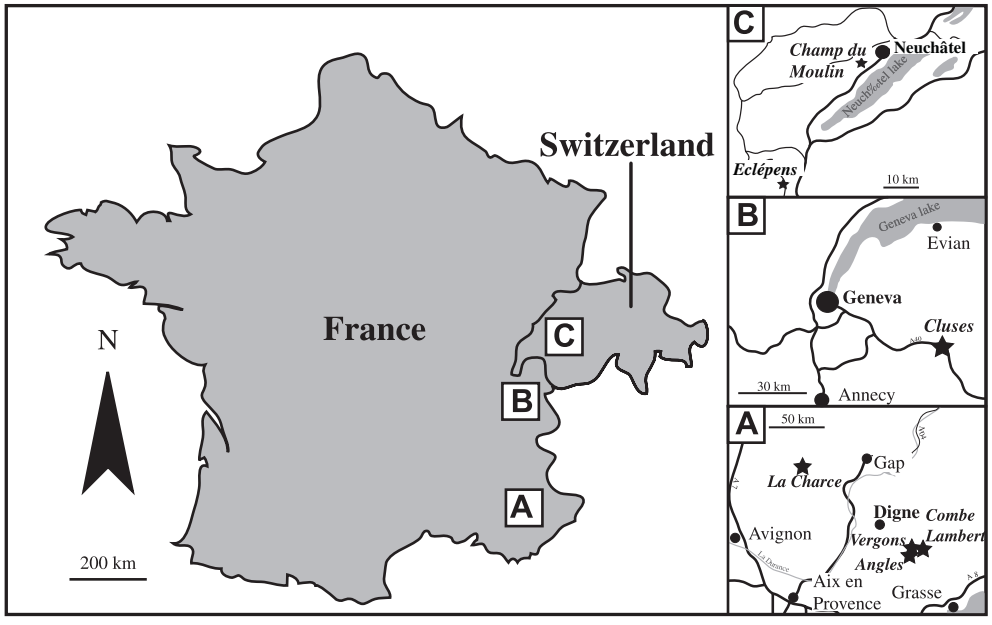

Fig. 1. Location of the studied sections.

3. Methods

3.1. Rock-Eval analysis

Organic matter analyses were performed using a Rock Eval 6 equipment at the Institute of Geology of the University of Neuchâtel, on a batch of 26 marls around the Faraoni Level equivalent at Angles. Approximately 100 mg of ground and homogenised sample is subjected to a pyrolysis step followed by the complete oxidation of the residual sample (Espitalié et al. (1985), Lafargue et al. (1998) and Behar et al. (2001)). A FID detector measures the hydrocarbon released during pyrolysis, while CO_2 and CO are detected by infrared absorbance during both steps. In the here applied standard cycle for "whole rock," pyrolysis starts isothermally at 300 °C for 3 minutes, after which the sample is heated to 650 °C. The oxidation step starts isothermally at 400 °C (3 min) and then heats up to 850 °C. Organic carbon decomposition results in 4 main peaks: the S1 (hydrocarbons released during the isothermal phase), the S2 (hydrocarbons produced between 300 and 650 °C), the S3 (CO_2 from pyrolysis of OM up to 400 °C), and the S4 peak (CO_2 released from residual organic matter below ca. 550 °C during the oxidation step). Mineral carbon decomposition is recorded by the S3′ (pyrolysis-CO_2 released above 400 °C), and the S5 peak (oxidation-CO_2 released above ca. 550 °C).

These peaks are used to calculate the amount of total organic carbon (TOC) and the amount of mineral carbon (MinC). In addition, the so-called hydrogen index (HI = S2/TOC) and oxygen index (OI = S3/TOC) are calculated. The HI and OI indices are proportional to the H/C and O/C ratios of the organic matter, respectively, and can be used for organic matter classification in Van-Krevelen-like diagrams (Espitalié et al., 1985).

Measurements are calibrated using two standards (IFP 160000 and VP143 h); the error relative to standard IFP 160000 is approximately 0.77, 0.08, 0.25 and 1.5 % for TOC, MinC, HI and OI, respectively.

3.2. XRD analysis

X-ray diffraction analyses were performed to identify and quantify the different components of the bulk rock (Angles) and the clay-mineral assemblages (all studied sections). As data for the upper part of Eclépens (Blanc-Aletru, 1995), Cluses (Wermeille, 1996), Vergons and La Charce (van de Schootbrugge, 2001) sections were obtained using the methods described by Kübler (1987) and Adatte et al. (1996), the same procedures were performed on samples from Angles, Combe-Lambert and the lower part of Eclépens. This allowed us to better compare the integrity of the dataset and to avoid discrepancies due to the process of quantification. Moreover, the methods described in these aforementioned papers are accurate enough for bulk rock composed of several different mineral phases, even if the procedures mentioned by Środoń (1980) and Hillier (1989) are known to be precise and have been subsequently used to analyse the bulk-rock composition.

Samples were trimmed to avoid altered material. Subsequently, they were roughly crushed in a "jaw" crusher, and an aliquot of the resulting gravels was crushed using an agate mortar to obtain a fine and homogeneous powder (grain size ≤ 40 μm).

3.2.1. Bulk-rock analysis

About 800 mg of the powder were pressed (20 bar) in a powder holder, and the bulk-sample was analysed by XRD at the Institute of Geology of the University of Neuchâtel (Scintag XRD 2000 Diffractometer), in order to determine bulk-rock mineralogy using procedures described by Ferrero (1965, 1966); Klug and Alexander (1974); Kübler (1983), and Adatte et al. (1996). This method allows the semi-quantification of the whole-rock mineralogy (obtained by XRD patterns of random powder samples) by using external standards with an error varying between 5 and 10% for the phyllosilicates and 5% for grain minerals. The different minerals recognized and quantified are calcite, "phyllosilicates" group, quartz, sodic plagioclase (albite), and potassic feldspar (microcline); the position of the peaks used for their recognition is given in Table 1. Organic matter, poorly crystallised minerals (such as pyrite and goethite), ankerite and dolomite were not quantified due to the low intensity of their respective peak. They constitute the unquantified component of the samples.

3.2.2. Clay mineral analysis

This procedure is based on the method described by Kübler (1987) and Adatte et al. (1996). Samples are transferred into glass

Table 1
Synthesis of the results of bulk-rock analysis performed on samples from Angles. All values in percents

Section	Age	Mineral	Peak position (°2θ)	Bulk rock					
				Marls		Limestones		All lithologies	
				Mean value	Extreme values	Mean values	Extreme values	Mean values	Extreme values
Angles	Part I	Calcite	29.43	51.80	19.8–78.8	82.10	68.1–91.5	66.00	19.8–91.5
		Quartz	26.65	9.50	2.5–14.4	4.30	2.6–6.5	7.10	2.5–14.4
		Phyllosilicate	19.80	16.20	7.2–32.6	3.90	0.0–8.1	10.40	0.0–32.6
		K-Feldspars	27.50	0.70	0.0–2.2	0.00	0.0–0.3	0.40	0.0–2.2
		Na-Plagioclases	27.90	1.00	0.0–2.1	0.10	0.0–0.6	0.60	0.0–2.1
		Unquantified	–	20.70	0.4–53.2	9.60	0.1–28.5	15.50	0.1–53.2
		Detrital Index	–	1.40	0.3–3.8	5.40	2.1–10.8	3.30	0.3–10.8
	Part II	Calcite	29.43	42.20	7.4–72.7	80.90	59.9–96.9	68.70	7.4–96.9
		Quartz	26.65	9.50	3.0–19.2	2.40	1.0–4.8	4.60	1.0–19.2
		Phyllosilicate	19.80	18.80	6.9–41.3	3.00	0.0–7.7	8.00	0.0–41.3
		K-Feldspars	27.50	0.60	0.0–1.9	0.00	0.0–0.4	0.20	0.0–1.9
		Na-Plagioclases	27.90	1.50	0.2–4.9	0.00	0.0–0.3	0.50	0.0–4.9
		Unquantified	–	26.90	1.1–61.5	13.70	0.0–37.8	17.90	0.0–61.5
		Detrital Index	–	1.00	0.1–2.7	6.30	1.5–30.8	4.60	0.1–30.8
	Part III	Calcite	29.43	53.40	35.2–72.3	81.10	67.3–91.1	70.50	35.2–91.1
		Quartz	26.65	11.20	8.0–15.2	4.40	2.5–7.6	7.00	2.5–15.2
		Phyllosilicate	19.80	17.90	8.0–22.4	3.40	0.0–9.0	9.00	0.0–22.4
		K-Feldspars	27.50	0.30	0.0–1.2	0.10	0.0–0.4	0.20	0.0–1.2
		Na-Plagioclases	27.90	0.90	0.9–2.8	0.10	0.0–0.3	0.40	0.0–2.8
		Unquantified	–	15.70	0.8–33.7	11.10	0.1–28.5	12.90	0.1–33.7
		Detrital Index	–	1.30	0.6–2.6	5.50	2.1–10.7	3.90	0.6–10.7

containers with de-ionised water and agitated by air injection; subsequently they are decarbonatized by HCl 10% (1.25 N) leaching during 20 min. Dissolution of the samples is promoted by ultrasonic disaggregation (3 minutes per sample). The insoluble residue is washed and centrifuged until a neutral suspension is obtained (pH 7–8). Using the Stokes law, two granulometric fractions are separated (<2 μm and 2–16 μm). The selected fraction is then pipetted and deposited on a glass plate. A first analysis is performed after air-drying at temperature room, a second one after saturation of the sample with ethylen-glycol, in order to identify swelling minerals, and a third one after heating to 350 °C for selected samples. The intensities of the identified minerals are measured for a semi-quantitative estimate of the proportion of clay minerals, which is therefore given in relative percent without correction factors for both fractions.

Mica, kaolinite, chlorite, illite / smectite irregular mixed-layers (R0), and ordered mixed-layers (R1) were identified in the studied sections; the position of the peaks used for their recognition is given in Table 2. Measurements of the amount of smectite and illite layers in the R0 mixed-layers were performed on both limestones and marls, following the procedure of Moore and Reynolds (1997; Table 3). They reveal the presence of two types of R0 minerals. The first one contains more than 80% of smectite layers, and corresponds to an almost pure smectite characterized by a peak at 5.2 °2θ; it will hereafter be called "smectite". The second type is characterized by less than 70–60% of smectite layers and by a peak (001) between 9 and 9.5 °2θ: the term R0 I/S will be used hereafter for such mineral. The R1 mixed-layers are corrensite (chlorite/smectite R1 mixed-layer) or rectorite (illite/smectite R1 mixed-layer). The illite cristallinity index (IC) was measured on several diffractograms of marls and limestones, following the methods described by Kübler (1987), and by Kübler and Goy-Eggenberger (2001).

4. Results

4.1. The Angles and Combe-Lambert sections

4.1.1. XRD analysis

For the Angles section, analyses of whole-rock (n = 180) and insoluble-residue (n = 170) samples were performed both on marl and limestone samples, whereas in sediments from the Combe-Lambert section, only clay minerals were analysed (n = 25).

Calcite content shows no major variations, except for samples belonging to the *Balearites balearis* and *Spathicrioceras angulicostatum* (Late Hauterivian), and to the *Holcodiscus uhligi* and *Heinzia sayni* ammonite zones (early Late Barremian), where significant drops in the calcite content are observed (Fig. 2). The quartz content decreases slightly from the base of the section up to the sedimentary interval attributed to the *Nicklesia pulchella* zone, and then it increases up to the top of the section, which belongs to the lower Aptian. The evolution of phyllosilicates follows that of quartz, with a rapid increase just below the Faraoni Level equivalent (at 24.50 m).

From these results, a detrital index (DI), which corresponds to the ratio of the calcite to the quartz and phyllosilicates (in percents), is calculated, assuming that the major part of quartz is of detrital origin, as suggested by the absence of any post-depositional silicification.

High DI values reflect low detrital input. The evolution of the DI can be divided into three parts (Fig. 2; see also Table 1):

I. From the base of the section to the Faraoni Level equivalent (*S. angulicostatum–Pseudothurmannnia mortilleti* boundary), DI values are low.
II. From the Faraoni Level equivalent to the sequence boundary (Sb) B4 (approximately at 109 m, in sediments of the *Hemihoplites feraudianus* ammonite zone; after Arnaud, 2005), the DI curve increases sharply.
III. From the SbB4 to the top of the section, the DI decreases to values comparable to those observed in part I.

In the insoluble residue of the <2 μm fraction of sediments from the Angles and the Combe-Lambert sections, mica, kaolinite, "smectite," chlorite, and R0 I/S were identified(Fig. 3; see also Table 2 and Fig. 6 for an example of diffractograms).

The evolution of the kaolinite/mica and kaolinite/smectite ratios points out the predominance of kaolinite relative to smectite and mica in certain intervals (Fig. 3). In particular, the kaolinite content reaches 25% of the total clay-mineral content in selected marly samples of part II of the section, whereas this mineral content tends to decrease in part III of the section. However, kaolinite remains relatively low in limestone samples, trough the entire section (see Table 2). Contrary to kaolinite, "smectite" is the most abundant mineral in part I and especially in part III of the Angles section, where it reaches a maximum of approximately 80% in sediments belonging to the *Martelites sarasini* zone. Whereas the evolution of mica is rather monotonous, the chlorite content increases gently from the base to the top, with higher contents in limestones (mean value of 21%) compared to those of marls (mean value of 11%); the repartition of the "smectite" follows the same rule, with higher contents in limestones compared to marls (mean values of 27% and 12%, respectively).

4.1.2. Rock Eval analysis

A batch of 26 samples of marl belonging to the time span from the *B. balearis* to the *Avramidiscus kiliani* ammonite zone were analysed for their organic geochemistry parameters (Table 4). The TOC values range from 0.35 to 2.63%, with a maximum reached in the *B. balearis* ammonite zone, under the Faraoni Level equivalent. The HI values are relatively low within the dataset, but an increase in noted around the Faraoni Level equivalent, with a maximum of 345 mgHC/gTOC. Finally, the measured T_{max} are somewhat high, with a mean value of 436 °C (extreme values of 432 and 440 °C).

4.2. The Cluses section

In contrast to the Angles and Combe-Lambert sections, smectite is absent in the analysed clay-mineral assemblage of this section: only mica, kaolinite, chlorite and mixed-layer clay minerals were identified (n = 194, Fig. 4; see also Table 2 and Fig. 6 for an example of diffractograms). In some samples, the nature of the mixed-layers has been identified: corrensite and rectorite are characterized by peaks at 6.0 and 6.5 °2θ, respectively, and sometimes by a superstructure near 3 °2θ which appears on diffractograms of glycolate-saturated samples. As these minerals are absent in most of the samples, they were not included in the quantification calculation (except for the samples illustrated by their diffractogram in Fig. 6).

In the Cluses section, some narrow intervals are enriched in kaolinite at the base and the top of the depositional sequence Ba4; then, a major episode of enrichment in this mineral is noted from the base of the Ba5 sequence upward, with maximum values reaching more than 50%. Kaolinite contents remains also high in sediments of Aptian age. This trend in kaolinite contents is also well expressed in the curves of the kaolinite/mica and kaolinite/(Qz + Fk + Pl) ratios (Fig. 4; see also Table 2).

4.3. The Eclépens section

Mica, kaolinite, "smectite," chlorite, and R0 I/S were identified in the <2 μm fraction of sediments from Eclépens (n = 186 in Fig. 5; see also Table 2 and Fig. 6 for an example of diffractograms).

Table 2
Synthesis of the results of insoluble residue (<2 μm) analysis performed on samples from Angles, Combe-Lambert, Cluses, and Eclépens. All values in relative percents

Section	Age	Mineral	Peak position (^{0}20)	Clay fraction(<2 μm)					
				Marls		Limestones		All Lithologies	
				Mean value	Extreme value	Mean value	Extreme value	Mean value	Extreme value
Angles 1 Combe-Lambert	Late Hautervian	Illie-Micas	8.8(001)	58	30–81	41	17–68	48	17–81
		Kaolinite	12.34 (001)/24.9 (002)	6	0–25	5	0–15	5	0–25
		"Smectite"	5.2 (001 on glycolated sample)	6	0–38	28	4–58	23	0–58
		Chlorite	12.34 (002)/25.2 (004)	8	0–23	18	6–38	13	0–38
		RO I/S	9–9.5 (001)	11	0–19	9	0–17	10	0–19
	Barremian	Illie-Micas	8.8(001)	51	25–73	36	6–74	41	6–82
		Kaolinite	12.34 (001)/24.9 (002)	20	0–51	8	0–19	11	0–51
		"Smectite"	5.2 (001 on glycolated sample)	12	2–25	23	2–78	19	0–78
		Chlorite	12.34 (002)/25.2 (004)	8	0–23	25	0–61	19	0–61
		RO I/S	9–9.5 (001)	10	1–25	9	3–21	9	1–25
	Earliest Aptian	Illie-Micas	8.8(001)	54	29–82	29	0–63	39	0–71
		Kaolinite	12.34 (001)/24.9 (002)	9	3–52	3	0–23	6	0–52
		"Smectite"	5.2 (001 on glycolated sample)	8	0–21	42	12–76	28	0–76
		Chlorite	12.34 (002)/25.2 (004)	19	3–56	11	0–55	15	0–56
		RO I/S	9–9.5 (001)	11	3–21	14	0–26	12	0–26
Cluses	Not attributed	Illie-Micas	8.8(001)	No limestone-marl alternation				94	80–100
		Kaolinite	12.34 (001)/24.9 (002)					3	0–19
		Chlorite	12.34 (002)/25.2 (004)					1	0–12
		RO I/S	9–9.5 (001)					3	0–20
	Barremian	Illie-Micas	8.8(001)					89	23–100
		Kaolinite	12.34 (001)/24.9 (002)					9	0–77
		Chlorite	12.34 (002)/25.2 (004)					2	0–36
		RO I/S	9–9.5 (001)					1	0–12
	Aptian	Illie-Micas	8.8(001)					76	0–100
		Kaolinite	12.34 (001) /24.9 (002)					20	0–100
		Chlorite	12.34 (002)/25.2 (004)					3	0–45
		RO I/S	9–9.5 (001)					1	0–10
Eclepens	Early Hauterivian	Illie-Micas	8.8(001)					59	28–100
		Kaolinite	12.34 (001)/24.9 (002)					3	0–15
		"Smectite"	5.2 (001 on glycolated sample)					25	0–60
		Chlorite	12.34 (002)/25.2 (004)					2	0–8
		RO I/S	9–9.5 (001)					11	0–20
	Not attributed	Illie-Micas	8.8(001)					53	22–100
		Kaolinite	12.34 (001)/24.9 (002)					1.5	0–8
		"Smectite"	5.2 (001 on glycolated sample)					25	0–62
		Chlorite	12.34 (002)/25.2 (004)					1.5	0–6
		RO I/S	9–9.5 (001)					19	0–70
	Late Barremian	Illie-Micas	8.8(001)					31	0–100
		Kaolinite	12.34 (001)/24.9 (002)					32	0–100
		"Smectite"	5.2 (001 on glycolated sample)					18	0–67
		Chlorite	12.34 (002)/25.2 (004)					5	0–16
		RO I/S	9–9.5 (001)					14	0–100

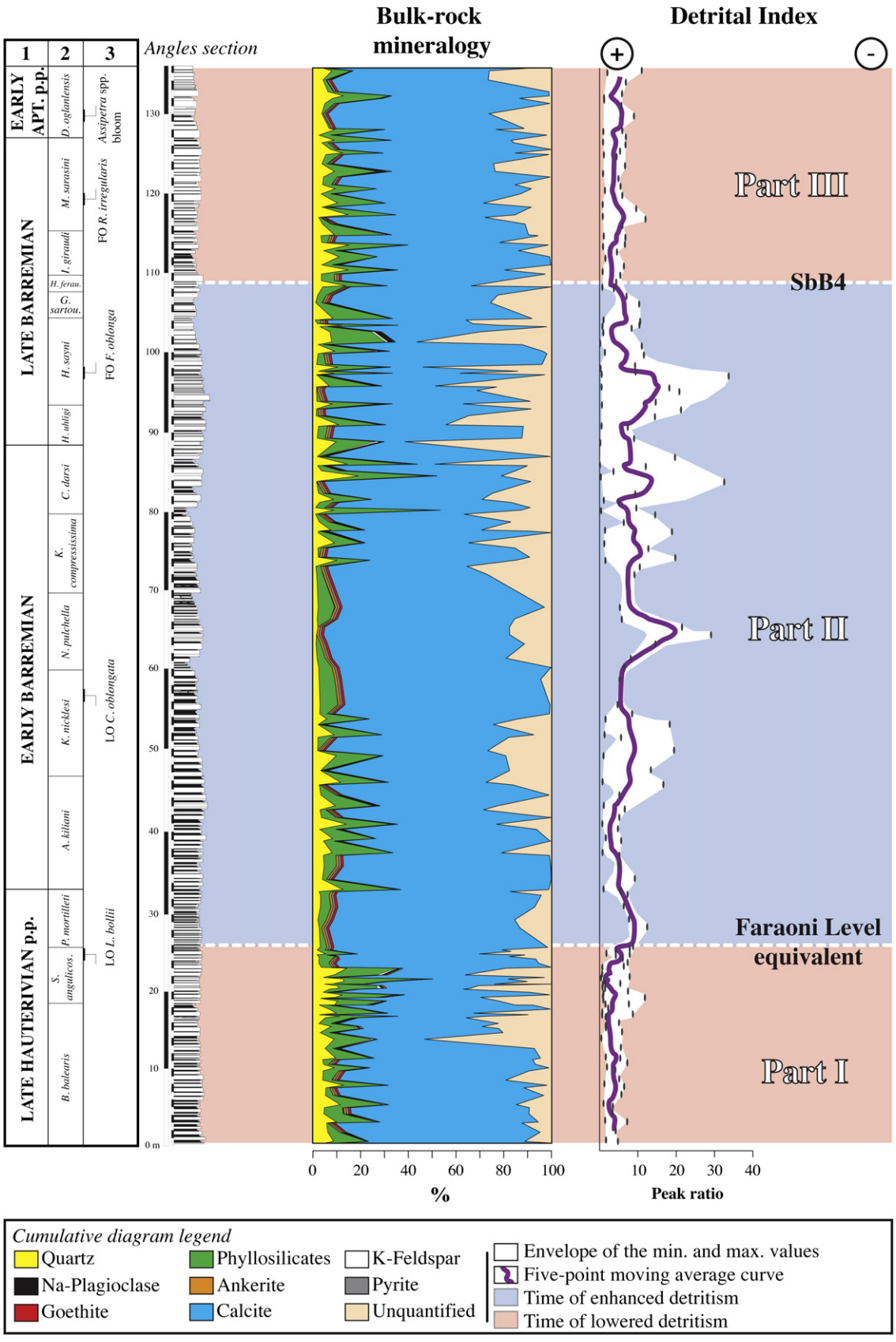

Fig. 2. Bulk-rock mineralogy of the Angles section. The detrital index corresponds to the ratio of calcite to quartz and phyllosilicates (in percentage). Numbers on top of the columns (left part of figure) correspond to the (1) stratigraphic stages, (2) ammonite zones and (3) main nannofossils bioevents (after Godet et al., 2006). The sequence boundary B4 (SbB4) is positioned after Arnaud (2005).

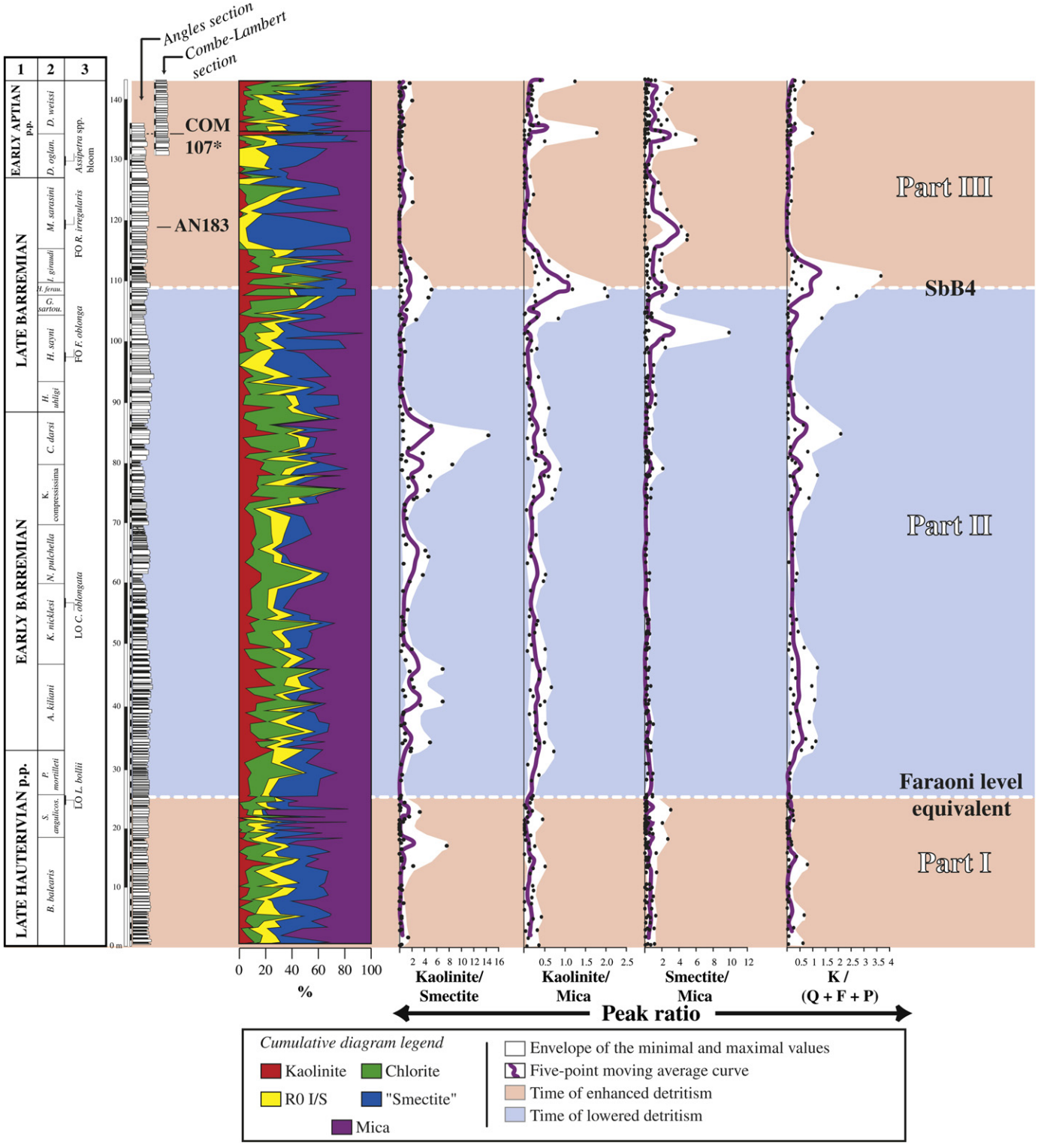

Fig. 3. Evolution of the clay-mineral assemblage of the insoluble residue (<2 μm fraction) of the Angles and the Combes-Lambert sections. On the right, the curves of the kaolinite/smectite, kaolinite/mica, and kaolinite/(quartz + feldspar + phyllosilicate) ratios point out the dominance of kaolinite during most of the Barremian. Numbers on top of the columns (left part of figure) correspond to the (1) stratigraphic stages, (2) ammonite zones and (3) main nannofossils bioevents (after Godet et al., 2006). Sample numbers refer to the diffractograms C and D displayed in Fig. 6. Abbreviations of the minerals: K = Kaolinite: Q = Quartz; F = potassic feldspar; P = sodic plagioclase.

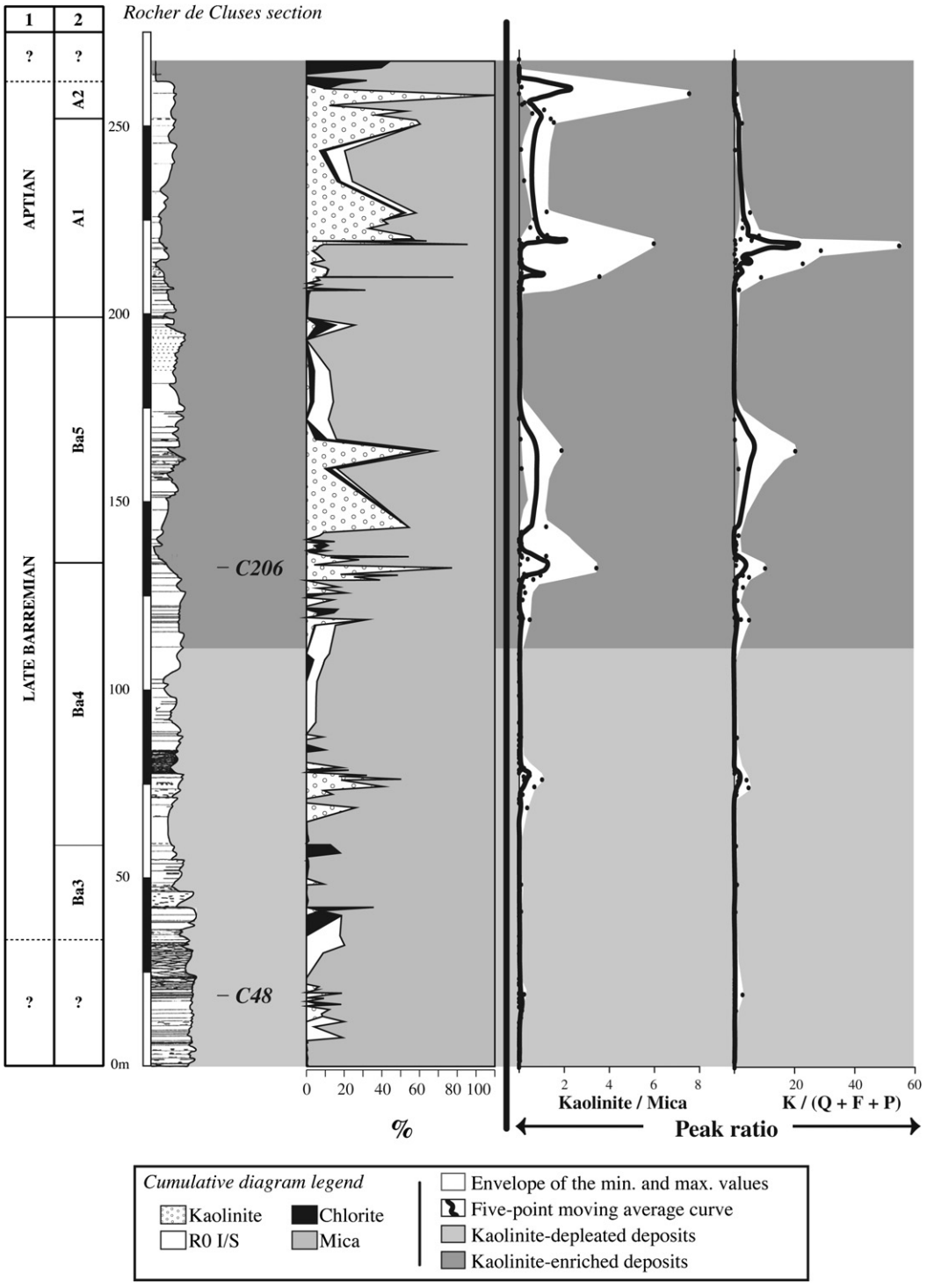

Fig. 4. Evolution of the clay-mineral assemblage of the insoluble residue (<2 μm fraction) of the Cluses section. On the left part of the figure, the numbers on top of the columns correspond to the (1) stratigraphic stages and (2) depositional sequences (after Wermeille, 1996). On the right, the evolution of the kaolinite/mica and kaolinite/(quartz + feldspar + phyllosilicates) ratios reveals the dominance of kaolinite from the upper part of the Ba4 depositional sequence (Late Barremian) to the top of the section (A2 sequence, lower Aptian). Sample numbers refer to the diffractograms E and F displayed in Fig. 6. Abbreviations of the minerals: K = Kaolinite: Q = Quartz; F = potassic feldspar; P = sodic plagioclase.

The most characteristic feature of the clay assemblage in this section is the antagonistic behaviour of ''smectite'' and kaolinite contents: ''smectite'' contents vary from 50% in the PJN to 0% in the UB, whereas kaolinite is mostly absent in the PJN and only appears in sediments above the boundary between the PJN and the UJ, with values reaching more than 50%.

5. Discussion

5.1. Reliability of the clay-mineral record

Clay minerals are formed in terrestrial soils, and have the potential to be subsequently eroded and exported to the ocean. Their genesis depends both on the lithological characteristics of the

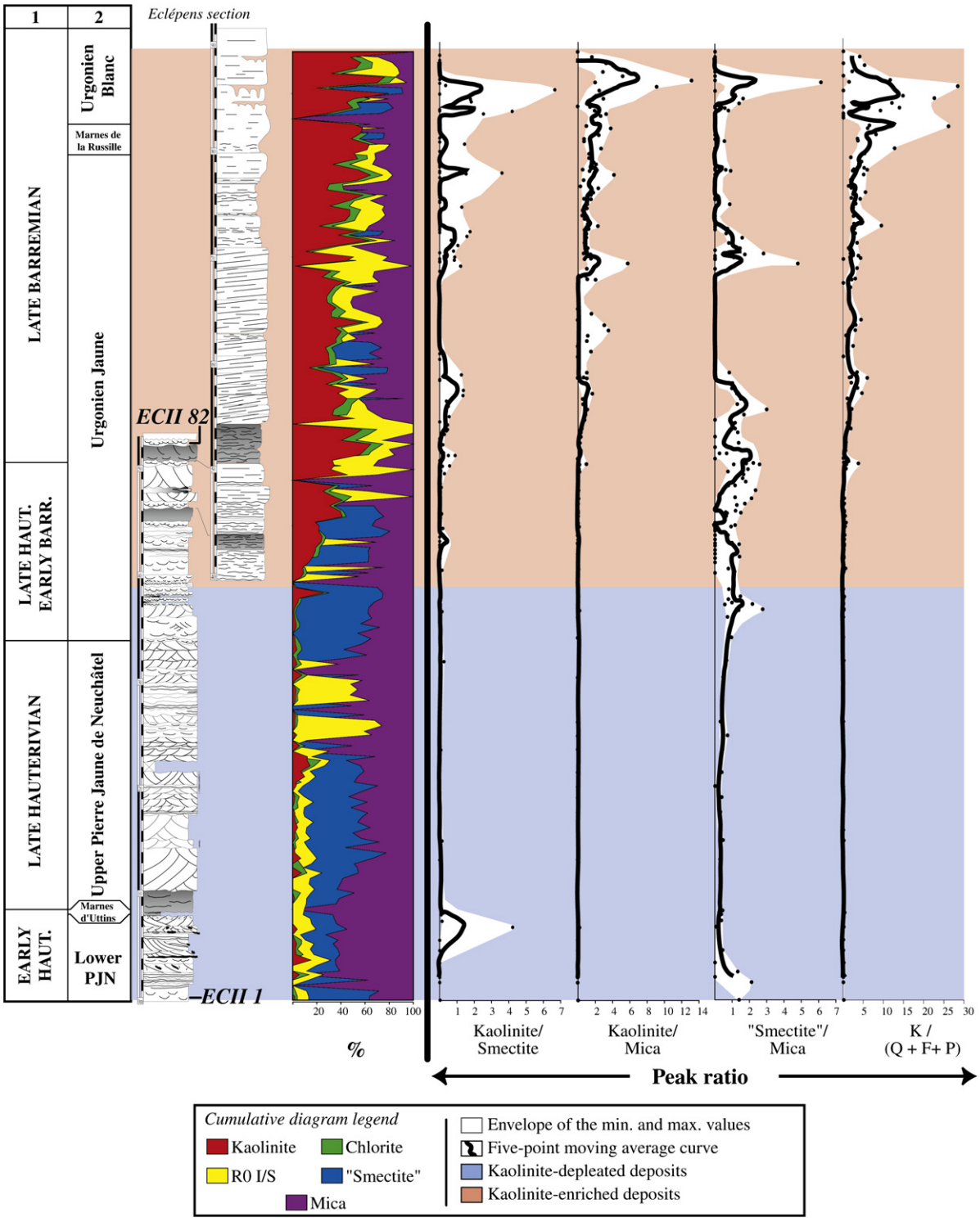

Fig. 5. Evolution of the clay-mineral assemblage of the insoluble residue (<2 μm fraction) of the Eclépens section. On the left part of the figure, the numbers on top of the columns correspond to the (1) stratigraphic stages (after Godet et al., 2005) and (2) formations. On the right, the curves of kaolinite/smectite, kaolinite/mica, and kaolinite/(quartz - + feldspar + phyllosilicate) ratios point out the dominance of the kaolinite throughout the Urgonian limestone, whereas sediments from the Pierre Jaune de Neuchâtel contain almost no kaolinite. Sample numbers refer to the diffractograms A and B displayed in Fig. 6. Abbreviations of the minerals: K = Kaolinite: Q = Quartz; F = potassic feldspar; P = sodic plagioclase.

substratum as well as on the prevailing climate. For example, smectite may form in soils exposed to a dry, seasonally well-contrasted climate or it may be also the result of the weathering of basalts (Chamley, 1989). Clay-mineral assemblages may then fractionate during their transport to the ocean - for example due to sea-level change and the shelf morphology, thereby perturbing the original environmental signal. Once deposited in the sedimentary environment clay-mineral compositions may be further modified by diagenetic processes (e.g., Chamley, 1989; Kübler and Jaboyedoff, 2000). The late diagenetic overprint is dependent on the original sediment composition, the degree of burial diagenesis and eventually also its tectonic history. Deconinck and Debrabant (1985)

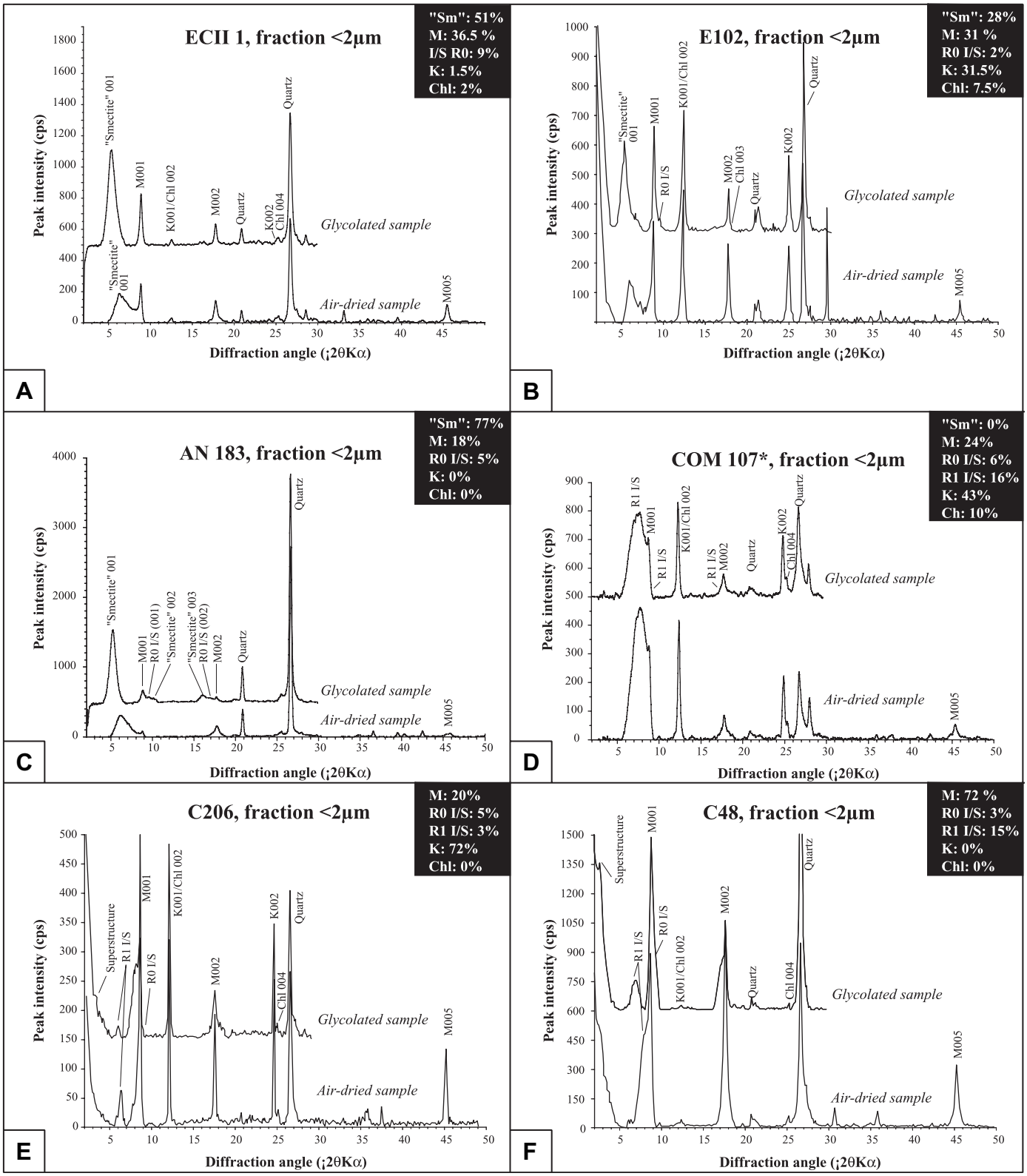

Fig. 6. Diffractograms characteristic of the studied sections. A, sample $EC_{II}1$ (oolitic grainstone), lower Hauterivian, base of the Eclépens section; B, sample E102 (bioclastic packstone), Late Barremian Eclépens section; C, sample AN183 (hemipelagic mudstone), *M. sarasini* ammonite zone (Late Barremian), Angles; D, sample COM107* (hemipelagic marlstone), boundary between the *Deshayesites oglanlensis* and *D. weissi* ammonite zones (Early Aptian), Combe-Lambert; F, sample C45 (bioclastic packstone), base of the Cluses section; E, sample C206 (peloidal grainstone to packstone with large benthic foraminifera), top of the depositional sequence Ba4 (upper Barremian), Cluses. Abbreviations of the minerals: "Sm" = "Smectite"; Sm = Smectite; M = Mica; K = Kaolinite; Chl = Chlorite.

studied limestones-marls alternations of Berriasian age from the Vergons section (southeastern France), where smectite contained in marl would preferentially transform into illite (and to a lesser extend into chlorite), whereas in limestone smectite would mainly convert into chlorite. Moreover, smectite is very sensitive to high temperatures linked to the burial and/or the tectonic history of the region: Ferry et al. (1983) interpreted the transformation of smectite into chlorite in sediments belonging to the Valanginian of the Vocontian Trough as the result of increasing thermal diagenesis, which may have affected carbonates more strongly than marls. The diagenetic transformation of smectite is also accompanied by the appearance of mixed-layered minerals, such as in Tithonian–Berriasian sediments of the Vergons section and in sediments from the Early Cretaceous of the Daluis section (Deconinck and Debrabant, 1985). All these mechanisms fractionating and transforming clay mineral assemblages may led to a misreading of the original climatic signal. This implies that the integrity of the clay-mineral assemblage is to be tested before its interpretation as a signal of the prevailing climate and changes therein.

5.1.1. Angles and Combe-Lambert

During the Cenozoic, the alpine orogenetic phase led to the formation of thrusts sheets in sediments belonging to the Vocontian Trough, and in particular the formation of the "nappe de Dîgne" had an impact on the thermal evolution of the Hauterivian–Barremian succession in the sections of Angles and Combe-Lambert (e.g., van de Schootbrugge et al., 2000). The associated tectonic overprint of clay-mineral assemblages did not completely obliterate their environmental signal: both the preservation of high contents of "smectites" and kaolinite compared to R0 I/S, as well as the absence of regular mixed-layers indicate low to medium diagenetic overprint. This is coherent with the amount of illite layers within the R0 I/S, which reaches an average value of 30% in the Angles and Combe-Lambert sections (all lithologies).

On the other hand, the higher proportion of chlorite preserved in limestones compared to marls may have been the consequence of quite strong diagenetic overprint (e.g., Deconinck and Chamley, 1983; Deconinck, 1987). But, as "smectites" display a similar behaviour, a change from humid to dryer conditions between marls and limestones may have controlled, at least in part, the distribution of both chlorite and "smectites" between the two lithologies. This is in agreement with the content of R0 I/S, which remains the same whatever the lithology. The better preservation of "smectite" in limestones compared to marls may also be a function of the lithology: Burkhard (1988) and Huon et al. (1994) reported the presence of well-crystallised smectite in micrite from the Doldenhorn nappe (Helvetic Alps), which reached temperatures of 300 to 350 °C during at least 10 millions years; this suggests that the fine-grained, carbonated lithology constitutes a protection against thermal diagenesis, which is in contradiction with the conclusions of Ferry et al. (1983).

Moreover, the IC values are highly variable, ranging from 0.15 to 0.2 °2θ in limestones, and from 0.35 to 0.4 °2θ in marls, which corresponds to values typical for the diagenetic zones 1 to 3 of Kübler and Jaboyedoff (2000). However, the increase of the IC in marls is certainly due to a higher content of "smectite" and R0 I/S compared to limestones, which may enlarge the peak 001 of the mica. The apparent thickness of this peak may therefore reflect a mixture of detrital illite and of mixed-layers.

On the other hand, Rock-Eval analyses were performed on 26 marl samples belonging to the *B. balearis* (Late Hauterivian) to the *A. kiliani* zones (Early Barremian) of Angles. In Fig. 7, T_{max} values reach 440 °C (mean value of 436 °C), which is consistent with the values obtained in the Vergons section by Baudin et al. (1999), who concluded a low degree of thermal diagenesis for this section. This implies that the sedimentary succession may have reached the beginning of the potential oil window and the zone of transition of the smectite to the R0 I/S (Espitalié et al., 1985; see also Fig. 23 in Kübler, 1997).

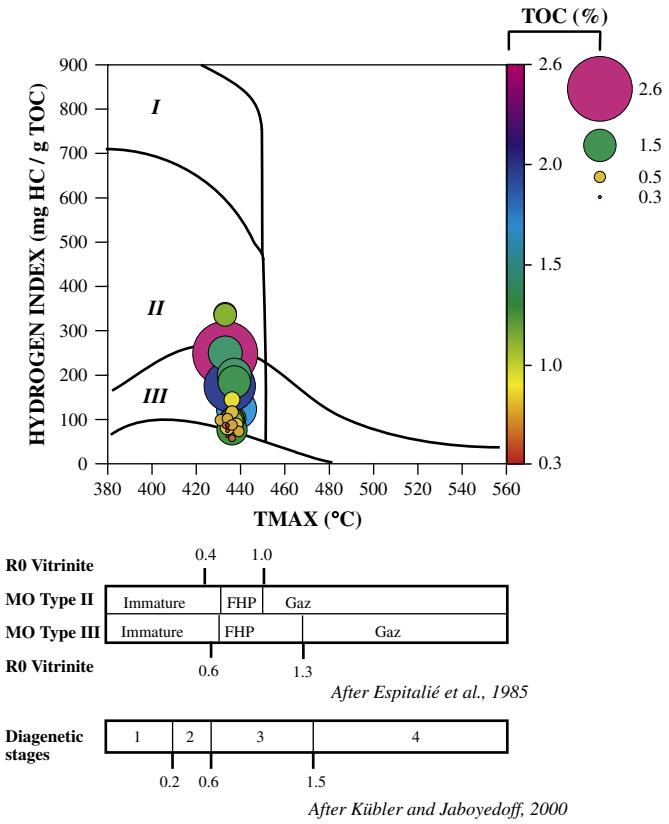

Fig. 7. Cross plot of the hydrogen index (HI) versus maximum of temperatures (T_{max}) for marls corresponding to the upper Hauterivian–lowermost Barremian interval of the Angles section. The shading and sizing of the bubbles corresponds to the total organic carbon (TOC) content. The evolution of kerogens and the correspondence of the diagenetic stages with respect to the reflectance of vitrinite is after Espitalié et al. (1985), and Kübler and Jaboyedoff (2000), respectively.

Finally, a recently published cross plot of $\delta^{13}C$ versus $\delta^{18}O$ measured at Angles (e.g., Wissler et al., 2002; Godet et al., 2006) reveals no clear correlation, and even if $\delta^{18}O$ displays relatively light values (minimum of −4.5‰ in Wissler et al., 2002), the trends observed in the stratigraphic evolution of $\delta^{18}O$ values at Angles can be correlated between the Vocontian Trough, the Ultrahelvetic realm in Switzerland and the Umbria-Marche basin in Italy, which excludes a strong diagenetic overprint at Angles (Godet et al., 2006).

All these parameters constrain the diagenetic overprint at Angles (and by extension at Combe-Lambert) close to the transition between stages 2 and 3 of Kübler and Jaboyedoff (2000). This implies that the main part of the clay-minerals assemblage is well-preserved in this succession, especially the kaolinite may have not suffered from diagenesis.

5.1.2. Cluses and Eclépens

At Cluses, diagenesis was more pronounced than at Angles and Combe-Lambert, as is suggested by the absence of smectite and the presence of rectorite and corrensite (Wermeille, 1996). However, the preservation of kaolinite suggests that the sedimentary succession underwent diagenetic overprint from the transition between stage 2 and 3 to the middle of the stage 4.

At Eclépens, the mineralogy of the clay fraction is more diversified, and includes some true smectites. This implies that diagenesis had a relatively low impact on the sedimentary succession, as is suggested by the rapid exhumation of the succession after a maximum burial depth of approximately 2500 m

Table 3
: Measurements of the content of smectite layers in samples from Angles, Combe-Lambert, and Eclépens. All values in percents

Section	Sample	Lithology	$\triangle 2\underline{\theta}$	% smectitic layers	% illitic layers
Angles	AN 2b	marlstone	6.22	61.05	39.07
	AN 6b	marlstone	5.76	76.99	23.11
	AN 10b	marlstone	6.26	59.72	40.40
	AN 15.1b	marlstone	5.93	71.06	29.04
	AN 18b	marlstone	6.93	39.75	60.39
	AN 29b	marlstone	6.69	46.44	53.69
	AN 34b	marlstone	6.51	51.75	48.38
	AN 38b	marlstone	6.51	51.79	48.34
	AN 81b	marlstone	6.15	63.26	36.86
	AN 103b	marlstone	6.21	61.29	38.83
	AN 35	limestone	5.67	80.69	19.40
	AN 49.1	limestone	5.40	91.17	8.92
	AN 156.4	limestone	5.64	81.67	18.43
	AN 156.6	limestone	5.97	69.54	30.56
	AN 181	limestone	5.46	88.79	11.30
	AN 183	limestone	5.70	79.52	20.58
	AN 185	limestone	5.76	77.12	22.98
	AN 190	limestone	5.85	73.81	26.30
	AN 197	limestone	5.37	92.36	7.73
	AN 206	limestone	5.19	100.01	0.07
	Mean values:		Marlstone	58.31	41.81
			Limestone	83.41	16.63
			All lithologies	70.89	29.22
Combe-Lambert	COM108*	marlstone	6.14	63.59	36.52
	COM 122*	marlstone	6.45	53.71	46.42
	COM 104	limestone	6.18	62.37	37.75
	COM 106	limestone	6.03	67.51	32.60
	COM 112	limestone	5.70	79.49	20.61
	COM 122 h	limestone	5.94	70.43	29.68
	COM 124	limestone	5.89	72.40	27.70
	Mean values:		Marlstone	58.65	41.47
			Limestone	70.44	29.67
			All lithologies	67.07	33.04
Eclepens	ECII 1	limestone	5.57	84.36	15.73
	ECII 3	limestone	5.69	79.67	20.43
	ECII 8	limestone	5.77	76.64	23.46
	ECII52	limestone	6.75	44.75	55.38
	ECII 55	limestone	5.76	77.24	22.86
	ECII 57	limestone	6.00	68.59	31.51
	ECII 60	limestone	6.00	68.61	31.50
	ECII 74	limestone	6.18	62.33	37.78
	ECII 82	limestone	5.70	79.42	20.68
	Mean values:		All lithologies	71.29	28.82

(Burkhard and Sommaruga, 1998). Moreover, the IC ranges between 0.25 and 0.3 °2θ (Blanc-Aletru, 1995); this implies that the majority of the mica from Eclépens has a detrital origin. Finally, the relative high content of smectite layers in R0 I/S (average value of approximately 71%; see Table 3) is another argument to conclude that the intensity of diagenesis did not exceed the middle of the diagenetic stage 2 of Kübler and Jaboyedoff (2000).

5.2. Climate change during the late Hauterivian–early Aptian

A correlation based of the stratigraphic evolution of kaolinite is proposed between the Western Swiss Jura, the Subalpine Chains, and the Vocontian Trough, for the time period from the Early Hauterivian to the earliest Aptian (Fig. 8). Kaolinite/smectite and smectite/mica ratios curves are also reported, where appropriate. In southeastern France and in the vicinity of Neuchâtel, clay-mineral assemblages are dominated by smectite during the Hauterivian. The lack of good age control at the base of the Cluses section, as well as diagenetic processes that may have transformed eventually present smectite into mixed-layer minerals, do not allow a firm correlation of this section with the two other domains for this interval.

In general, the dominance of "smectites" from the base of the Hauterivian stage to the *B. balearis* ammonite zone (mean value of 59%; extreme values of smectite for this interval: 20 to 81%), suggests the presence of a dry but seasonally contrasted climate (e.g., Chamley, 1989; Weaver, 1989).

Upwards, the evolution in kaolinite contents follows a threefold division, with low values in part I and III and an increase in part II; the same behaviour is reported for the evolution of the kaolinite/mica and the kaolinite/(quartz + feldspar + plagioclase) ratios. Kaolinite constitutes therefore the main mineral of the clay assemblage in the sections of Angles and Combe-Lambert for most of the Barremian. This conclusion is supported by the clay-mineral evolution from the Cluses section (Fig. 4).

The presence of kaolinite implies a warm or humid climate, under which well-drained continental areas may undergo intense biogeochemical weathering leading to the concentration of Al_2O_3 and the genesis of bauxite and associated kaolinite (e.g., Chamley, 1989; Weaver, 1989; Thiry et al., 1999). In the time interval from the *P. mortilleti* to the *Imerites giraudi* ammonite zones, the development of such soils may have been important on the southern European continent bordering the northern Tethyan margin, due to a shift from a seasonally well contrasted to a warmer and more humid climate during the latest Hauterivian (Fig. 8). The stratigraphically highest peak in kaolinite content is observed in marly sediments near the SbB4 and this may reflect the predominance of

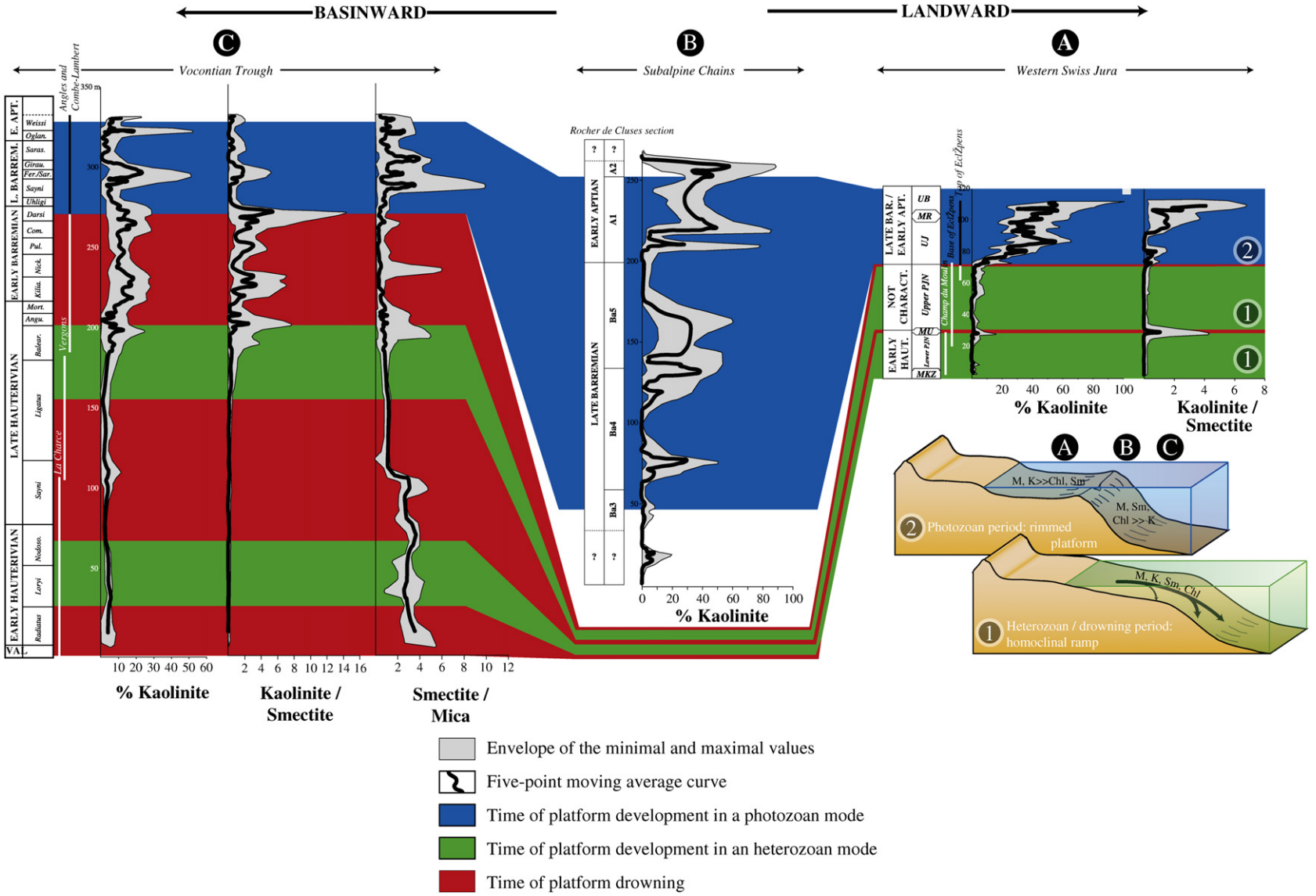

Fig. 8. Correlation between the Vocontian Trough (Angles and Combe-Lambert sections), the Subalpine Chains (Cluses section), and the Western Swiss Jura (Champ du Moulin and Eclépens sections), based on the kaolinite evolution. Both the relative abundance of kaolinite, as well as the kaolinite/smectite ratio are used, where appropriate. Bloc diagrams on the right side of the figure illustrate the morphology of the platform and the subsequent differential settling of clay-minerals during times of heterozoan and drowned platform (1), and photozoan platform (2); on the top on these two transects, the letters A, B and C indicate the theoretical position of the three studied regions along the margin. Note that data from Champ du Moulin (after Rumley, 1993; see Fig. 1 for a location) complete the data from Eclépens for the lower PJN. Abbreviations of formations names: MKZ: Mergelkalk zone; MU: Marnes d'Uttins; MR: Marnes de la Russille.

Table 4
: Results of the Rock Eval analyses performed on marls from the *B. balearis* to the *A. kiliani* ammonite zones (Angles section)

ID	Depth [m]	Stage	Ammonite Zone	TOC [%]	MINC [%]	HI [mgHC/g TOC]	OI [mgCO_2/g TOC]	Tmax [∞C]
AN29b	15.35	Late Hauterivian	*B. balearis*	0.39	8.03	82	137	435
AN30b	15.82	Late Hauterivian	*B. balearis*	0.65	6.74	94	84	437
AN31b	16.12	Late Hauterivian	*B. balearis*	0.47	7.54	93	95	434
AN32b	16.65	Late Hauterivian	*B. balearis*	2.63	3.20	254	35	434
AN33b	17.35	Late Hauterivian	*B. balearis*	1.49	4.76	207	73	438
AN34b	17.94	Late Hauterivian	*B. balearis*	0.35	9.15	70	129	435
AN35b	18.29	Late Hauterivian	*B. balearis*	0.71	7.51	123	113	437
AN37b	19.00	Late Hauterivian	*S. angulicostatum*	1.44	4.79	191	50	438
AN38b	19.47	Late Hauterivian	*S. angulicostatum*	1.08	5.29	101	83	437
AN39b	19.94	Late Hauterivian	*S. angulicostatum*	0.77	5.87	88	88	435
AN40b	20.41	Late Hauterivian	*S. angulicostatum*	1.14	5.06	104	85	437
AN41b	20.59	Late Hauterivian	*S. angulicostatum*	1.73	3.46	130	55	439
AN42b	21.00	Late Hauterivian	*S. angulicostatum*	1.15	4.99	106	65	437
AN43b	21.29	Late Hauterivian	*S. angulicostatum*	0.73	7.24	95	66	439
AN44b	21.59	Late Hauterivian	*S. angulicostatum*	0.65	6.17	80	84	440
AN45b	21.82	Late Hauterivian	*S. angulicostatum*	1.37	1.81	84	63	437
AN46b	22.35	Late Hauterivian	*S. angulicostatum*	2.13	1.89	181	51	436
AN48b	23.29	Late Hauterivian	*S. angulicostatum*	1.11	4.22	109	140	438
AN51b	24.53	Late Hauterivian	*S. angulicostatum*	1.09	10.18	345	42	434
AN52b	25.06	Late Hauterivian	*S. angulicostatum*	1.49	7.97	256	48	434
AN53.1b	25.18	Late Hauterivian	*S. angulicostatum*	1.09	1.16	342	45	434
AN72b	33.87	Early Barremian	*A. kiliani*	0.50	6.42	65	111	437
AN73b	34.43	Early Barremian	*A. kiliani*	0.65	5.42	109	69	435
AN74b	34.74	Early Barremian	*A. kiliani*	0.66	4.78	105	80	432
AN75b	35.37	Early Barremian	*A. kiliani*	0.82	5.19	151	44	437
AN76b	35.68	Early Barremian	*A. kiliani*	0.39	7.60	94	89	435

humid conditions during the deposition of marls. However, an intensification of humid conditions during the *H. sayni* and the *H. feraudianus* ammonite zones is also suggested by the symmetric shape of this increase around the SbB4.

A comparison with the $\delta^{18}O$ measured on bulk-rock limestone samples from the Angles section (Godet et al., 2006) suggests a possible link between the variations in temperature mirrored by the main trends of the $\delta^{18}O$ curve and the evolution of the kaolinite content (Fig. 9). Effectively, Godet et al. (2006) described a four-fold evolution, with two maxima in $\delta^{18}O$ values at the base of the *N. pulchella* and in particular in the *I. giraudi* ammonite zones. Whereas the first maximum in the $\delta^{18}O$ record corresponds to a period characterized by stable but relatively moderate kaolinite contents, the second maximum follows immediately after the highest values recorded in the kaolinite evolution. The genesis of kaolinite requires a humid and warm climate; in the part II of the Angles section, the augmentation in kaolinite content may mirror an increased continental runoff, which may have constituted a sink for atmospheric CO_2. Subsequently, the greenhouse effect may have decreased and the temperature as well. As a consequence, the $\delta^{18}O$ values may shift toward more positive values after episodes of high continental runoff, as the one recorded from the end of the *H. sayni* to the *I. giraudi* ammonite zones at Angles. Thereafter, the $\delta^{18}O$ returns to lighter values, reflecting an increase of temperature. Alternatively, the evolution of kaolinite is compatible with the $\delta^{18}O$ record, if the latter reflects salinity rather than temperature; during time of kaolinite dominance, the input of freshwater in the ocean may increase, as kaolinite genesis requires an increased rainfall. Consequently, the salinity of the surface ocean may decrease by dilution and the $\delta^{18}O$ may shift toward more negative values.

5.3. Kaolinite evolution from the Vocontian Trough to the western Swiss Jura: evidence for differential settling

The evolution of kaolinite contents along the northern Tethyan margin from the late Early Barremian to the earliest Aptian reveals an ambiguous behaviour of this clay mineral: whereas the Late Barremian sedimentary record in the Western Swiss Jura is characterized by high kaolinite contents (Fig. 6 and Table 2), contemporaneous sediments deposited in the Vocontian trough are relatively impoverished in this mineral (Fig. 4 and Table 2). As the kaolinite content displays intermediate values in upper Barremian—lower Aptian sediments from the Cluses section (Table 2), a link between sea-level fluctuation, a change in the morphology of the carbonate platform, and migration of the depo-centre of kaolinite as a function of the distance from the coastline through sea-level change may explain this apparent decrease in kaolinite in distal directions along the northern Tethyan margin.

During the Hauterivian, a heterozoan assemblage dominated the carbonate-producing community along the northern Tethyan margin, whereas during the period between the *C. darsi* (late Early Barremian) and the *Deshayesites weissi* ammonite zones (Early Aptian), this assemblage progressively evolved into a photozoan ecosystem (Föllmi et al., 1994, 2006). In the period between the latest Hauterivian and late Early Barremian (*P. mortilleti* to the *C. darsi* ammonite zone), the Helvetic platform underwent a major drowning phase (Bodin et al., 2006b). An important difference between these two regimes of carbonate production is associated with the platform morphology: the Hauterivian heterozoan platform is interpreted as a ramp structure with a good connection to the ocean, whereas the late Early Barremian to Early Aptian photozoan platform developed a marginal rim consisting of patch reefs and oolitic shoals (e.g., Arnaud-Vanneau, 1980). The heterozoan platform structure was, for this reason, particularly favourable to the bypass of detrital continental material, such as clay minerals and quartz particles, into the open sea. The photozoan platform structure may, on the contrary, have functioned as a barrier for larger detrital particles such as kaolinite, and may have fractioned the clay-mineral assemblage transferred to the ocean in a way that the larger, less reactive kaolinite particles were trapped on the platform (see below).

In the Vocontian Trough, kaolinite is absent in sediments older than the latest Hauterivian (data from van de Schootbrugge, 2001), appears in sediments attributed to the *B. balearis* ammonite zone and reaches more than 30–40% in lower Barremian sediments (Fig. 8). The absence of kaolinite and the dominance of smectite in most of the Hauterivian sediments may reflect a true climatic signal, which is in agreement with the type of carbonate platform

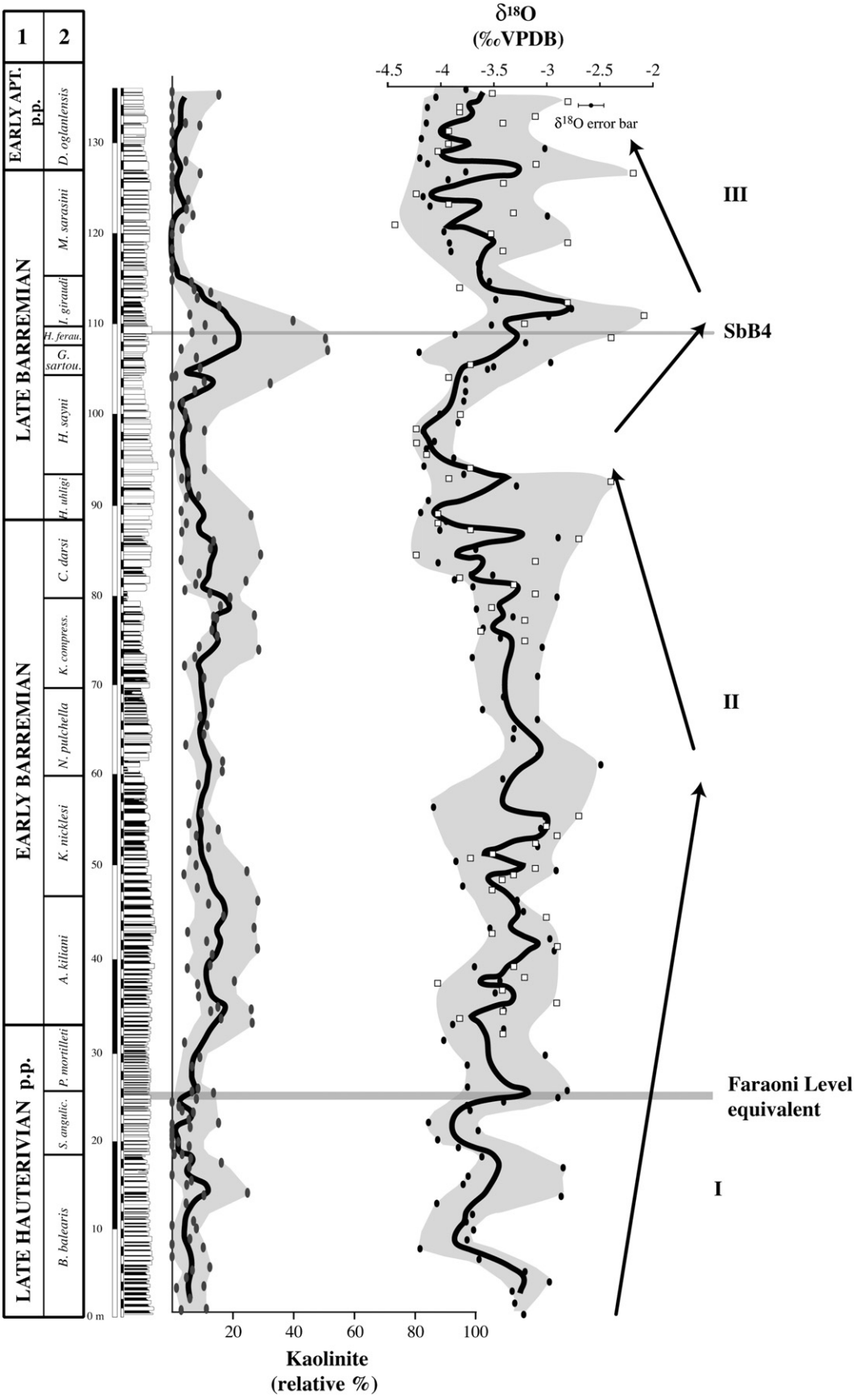

Fig. 9. Comparison of the kaolinite and the $\delta^{18}O$ (measured on bulk-rock limestone samples) evolution in the Angles section. On the left side of the figure, the numbers on the top of the columns corresponds to the stratigraphic stage (1) and the ammonite zone (2). The $\delta^{18}O$ values are after Wissler et al. (2002; white squares), and Godet et al. (2006; black circles).

that developed at that time, under high nutrient conditions (e.g., van de Schootbrugge et al., 2003; Bodin et al., 2006a). During the latest Hauterivian, the appearance of kaolinite indicates a change from a seasonally contrasted towards a more humid and warm (intertropical) climate that can be linked to an acceleration of the hydrologic cycle, and with that an increase in continental run-off. The related enhanced supply of phosphorus and of Dissolved Inorganic Carbon (DIC) to the ocean may have been triggered by intensified biogeochemical weathering, as already suggested by Bodin et al. (2006a) and Godet et al. (2006). The latter linked the very stable evolution of the $\delta^{13}C$ record observed from the base of the *P. mortilleti* to the top of the *C. darsi* ammonite zone to an increase of the oceanic DIC volume in the ocean, which may have buffered the $\delta^{13}C$ signal against paleoceanographic change (see Bartley and Kah (2004) for a detailed explanation of the DIC buffering effect on the $\delta^{13}C$ record). As a consequence of the change towards a warmer and wetter climate during the latest Hauterivian and a corresponding increase in phosphorus input into the ocean, the northern Tethyan carbonate platform drowned (during the period between the *S. angulicostatum* and the *C. darsi* ammonite zones; Arnaud-Vanneau and Arnaud, 1990; Bodin *et al.*, 2006b).

Then, from the *Gerhardtia sartousiana* ammonite zone onward, carbonate production took up again on the platforms of the northern Tethys, and this especially in the Vercors and the Helvetic Alps (Arnaud-Vanneau and Arnaud, 1990; Föllmi et al., 1994, 2006; Bodin et al., 2006c); corals, green algae, stromatoporoids and associated rudists recovered in the platform sediments of this period are typical of a photozoan assemblage (e.g., James, 1997; Mutti and Hallock, 2003). During the time of carbonate production in a photozoan mode, the presence of a barrier or a reef that separated the platform from the basin, as well as the morphology of the platform may have led to a fractionation of clay minerals during their transfer to the ocean. This is related to the size of kaolinite crystals (and consequently its weight) as well as its high capacity to flocculate (Ruffell et al., 2002), which both may have favoured the deposition of this mineral after a relatively brief transport in the ocean (e.g. Gibbs, 1977; Hallam, 1984), and may have led to a decrease of the kaolinite content toward the basin. Moreover, this differential settling of clay particles may have been enhanced by changes in sea-level. During sea-level rise and subsequent sea-level highstand, the shelf area increases and the distance between the continent where kaolinite was formed and the basin becomes more important. Moreover, the diversity and the development of facies susceptible to trap detrital particles are the highest within highstand deposits. This implies that kaolinite may be deposited in proximal shelf settings rather than in hemipelagic environments during periods of high sea-level. This may also explain the difference in the quantity of kaolinite deposited along the northern Tethyan margin during the Late Barremian and earliest Aptian, as this time span corresponds to a long-term maximum in eustatic sea level (Haq et al., 1987; Arnaud, 2005).

This fractionation pattern with regards to the kaolinite distribution in clay-mineral assemblages has already been suggested for the Valanginian-Hauterivian carbonate platform (Adatte and Rumley, 1989), and for the middle Jurassic succession (Bolle et al., 1996) of the Western Swiss Jura. Sediments from a platform developing in a photozoan mode may as a consequence record a faithful climatic signal, whereas in the adjacent hemipelagic setting the preserved clay-mineral assemblage may have been fractionated and the climate signal correspondingly altered. Consequently, looking at the clay-minerals evolution along a platform to basin transect may be more useful than considering only pelagic sections when attempting to trace climate change.

6. Conclusions

The evolution of clay-mineral assemblages during the Hauterivian, Barremian and earliest Aptian along a platform-basin transect in the northern Tethys highlights the dominance of smectite and the quasi absence of kaolinite in sediments up to the latest Hauterivian. During the latest Hauterivian to the Early Aptian, kaolinite becomes abundant, which may indicate a general change from a seasonally contrasted, temperate climate prevailing during the Hauterivian to a warmer and wetter climate in the period from the latest Hauterivian to the earliest Aptian for the southern European realm adjacent to the Northern Tethys. The increased humidity and enhanced continental runoff may have triggered elevated input of nutrients and DIC in the ocean. The latter may have contributed to initiate the anoxia characteristic of the Faraoni Level, and also to buffer the $\delta^{13}C$ signal.

The distribution of clay minerals along this transect was not only influenced by climate change, but also by the morphology of the platform and by sea-level change. During the Hauterivian, the ramp-type morphology of the northern Tethyan platform may have favoured a direct transport of clay particles into the basin without major fractionation. From the *B. balearis* to the *C. darsi* ammonite zone, the Helvetic platform underwent a major phase of drowning, which may have also facilitated the transport of clay toward the basin. The re-installation of the carbonate platform in a photozoan mode near the Early-Late Barremian boundary and the development of a marginally rimmed platform topography–together with general sea-level rise - may have fractionated the clay-mineral assemblages during their transport into the basin, with the preferred deposition of kaolinite in proximal settings, and the subsequent depletion of this mineral in distal environments. This highlights the importance of comparing several sections distributed along a proximal–distal transect, in order to better constrain climatic changes by means of clay mineralogy.

Acknowledgements

The authors acknowledge Laureline Scherler and Laurent Chalumeau (University of Neuchâtel) for the preparation of the samples from Angles with regards to the clay-mineral analysis, Philipp Steinmann (University of Neuchâtel) for performing the Rock Eval analyses, and Stéphane Westermann (University of Neuchâtel) for the help in sampling and measuring the Combe-Lambert section. We thank the staff of the Eclépens quarry (Holcim company), for allowing us to sample the Eclépens section. This research is financially supported by the Swiss National Fund (projects n°2100-067807/1 and 200020-105206/1). The reviews of Cédric John, Thomas Pletsch, and Alastair Ruffell greatly improved the quality of this manuscript.

References

Adatte, T., Rumley, G., 1989. Sedimentology and mineralogy of the Valanginian and Hauterivian in the stratotypic region (Jura mountains, Switzerland). In: Wiedmann, J. (Ed.), Cretaceous of the Western Tethys: proceedings of the 3rd International Cretaceous Symposium, Tübingen 1987. E. Schweizerbart'sche Verlagsbuchhandlung, Stuttgart, pp. 329–351.

Adatte, T., Stinnesbeck, W., Keller, G., 1996. Lithostratigraphic and mineralogic correlations of near K/T boundary sediments in northeastern Mexico: Implications for origin and nature of deposition. In: Ryder, G., Fastovsky, D., Gartner, S. (Eds.), The Cretaceous-Tertiary Event and Other Catastrophes in Earth HistoryGeological Society of America Special Paper 307, pp. 211–226.

Arnaud, H., 2005. The South-East France Basin (SFB) and Its Mesozoic Evolution. Géologie Alpine Série Spéciale "Colloques et Excursions" n°7, 5–28.

Arnaud-Vanneau, A., 1980. Micropaléontologie, paléoécologie et sédimentologie d'une plate-forme carbonatée de la marge passive de la Téthys: l'Urgonien du Vercors septentrional et de la Chartreuse (Alpes occidentales). Géologie Alpine Grenoble Mém HS 10, 874.

Arnaud-Vanneau, A., Arnaud, H., 1990. Hauterivian to Lower Aptian carbonate shelf sedimentation and sequence stratigraphy in the Jura and northern Subalpine chains (southeastern France and Swiss Jura). In: Tucker, M.E., Wilson, J.L.,

Crevello, P.D., Sarg, J.R., Read, J.F. (Eds.), Carbonate Platforms: Facies, Sequences and Evolution. Blackwell Scientific Publications, Special Publication of the International Association of Sedimentologists, 9, pp. 203–233.

Bartley, J.K., Kah, L.C., 2004. Marine carbon reservoir, C_{org} - C_{carb} coupling, and the evolution of the Proterozoic carbon cycle. Geology 32, 129–132.

Baudin, F., 2005. A late Hauterivian short-lived anoxic event in the Mediterranean Tethys: the "Faraoni Event". Comptes Rendus de l'Académie des Sciences de Paris 337, 1532–1540.

Baudin, F., Bulot, L.G., Cecca, F., Coccioni, R., Gardin, S., Renard, M., 1999. Un équivalent du "Niveau Faraoni" dans le Bassin du Sud-Est de la France, indice possible d'un événement anoxique fini-hauterivien étendu à la Téthys méditerranéenne. Bulletin de la Société géologique de France 170, 487–498.

Behar, F., Beaumont, V., De B. Penteado, H.L., 2001. Rock-Eval 6 technology: performances and developments. Oil & Gas Science and Technology - Rev. IFP 56, 111–134.

Berner, R.A., Kothavala, Z., 2001. Geocarb III: a revised model of atmospheric CO_2 over Phanerozoic time. American Journal of Science 301, 182–204.

Blanc-Aletru, M.C., 1995, Importance des discontinuités dans l'enregistrement sédimentaire de l'Urgonien jurassien. Micropaléontologie, Sédimentologie, Minéralogie et Stratigraphie Séquentielle, Géologie Alpine, Ph.D. Thesis Grenoble, Laboratoire de Géologie de l'Université I de Grenoble, 299 pp.

Bodin, S., Godet, A., Vermeulen, J., Arnaud, H., Strasser, A., Fiet, N., Adatte, T., Föllmi, K.B., 2006a. The late Hauterivian Faraoni oceanic anoxic event in the western Tethys: Evidence from phosphorus burial rates. Palaeogeography, Palaeoclimatology, Palaeoecology 235, 245–264.

Bodin, S., Godet, A., Vermeulen, J., Linder, P., Föllmi, K.B., 2006b. Biostratigraphy, sedimentology and sequence stratigraphy of the latest Hauterivian-early Barremian drowning episode of the Northern Tethyan margin (Altmann Member, Helvetic Nappes, Switzerland). Eclogae Geologicae Helvetiae 99, 157–174.

Bodin, S., Vermeulen, J., Godet, A., Föllmi, K.B., 2006c. New data on the age of the installation of Urgonian-type carbonates along the northern Tethyan margin: biostratigraphy of the Chopf Member (Helvetic Alps, eastern Switzerland). Comptes Rendus Geoscience 338, 727–733.

Bolle, M.-P., Adatte, T., Mangold, C., Remane, J., 1996. Microfaciès, minéralogie, stratigraphie du Dogger de la région du Furcil (NE). Bulletin de la Société neuchâteloise des Sciences Naturelles 119, 123–144.

Bulot, L.G., Thieuloy, J.-P., Blanc, E., Klein, J., 1992. Le cadre stratigraphique du Valanginien supérieur et de l'Hauterivien du Sud-Est de la France; définition des biochronozones et caractérisation de nouveaux biohorizons. Géologie Alpine 68, 13–56.

Burkhard, M., 1988. L'Helvétique de la bordure occidentale du massif de l'Aar (évolution tectonique et métamorphique). Eclogae Geologicae Helvetiae 81, 63–114.

Burkhard, M., Sommaruga, A., 1998. Evolution of the western Swiss Molasse basin: structural relations with the Alps and the Jura belt. In: Mascle, A., Puigdefâbregas, C., Luterbacher, H.P., Fernàndez, M. (Eds.), Cenozoic foreland Basins of Western Europe, 134. Geological Society Special Publications, pp. 279–298.

Cecca, F., Faraoni, P., Marini, A., Pallini, G., 1995. Field-trip across the representative sections for the upper Hauterivian-Barremian ammonite biostratigraphy in the Maiolica exposed at Monte Nerone, Monte Petrano and Monte Catria (Umbria-Marche, Apennines). Memorie Descrittive della Carta Geologica d'Italia 51, 187–211.

Chamley, H., 1981. Long-term trends in clay deposition in the ocean. Oceanologica Acta n°SP Proceedings 26th International Geological Congress, Geology of Oceans Symposium, Paris, July 7–17, 1980, 105–110.

Chamley, H., 1989. Clay sedimentology. Springer Verlag, Berlin, 623 pp.

de Montmollin, A., 1835. Mémoire sur le terrain Crétacé du Jura. Mémoires de la Société des Sciences Naturelles de Neuchâtel tome I, 49–65.

Deconinck, J.-F., 1987. Identification de l'origine détritique ou diagénétique des assemblages argileux: le cas des alternances marne-calcaire du Crétacé inférieur subalpin. t. III. Bulletin de la Société Géologique de France 8, 139–145.

Deconinck, J.-F., Chamley, H., 1983. Héritage et diagenèse des minéraux argileux dans les alternances marno-calcaires du Crétacé inférieur du domaine subalpin. Comptes Rendus de l'Académie des Sciences de Paris 297, 589–594.

Deconinck, J.-F., Debrabant, P., 1985. Diagenèse des argiles dans le domaine subalpin: rôles respectifs de la lithologie, de l'enfouissement et de la surcharge tectonique. Revue de Géologie Dynamique et de Géographie Physique 26, 321–330.

Delanoy, G., 1997. Biostratigraphie des faunes d'Ammonites à la limite Barrémien-Aptien dans la région d'Angles-Barrême-Castellane. Etude particulière de la famille des Heteroceratina Spath, 1922 (Ancyloceratina, Ammonoidea). Annales du Muséum d'Histoire Naturelle de Nice Tome XII, 1–270.

Espitalié, J., Deroo, G., Marquis, F., 1985. La pyrolyse Rock-Eval et ses applications. Revue de l'Institut Français du Pétrole 40, 563–579.

Ferrero, J., 1965. Dosage des principaux minéraux des roches par diffraction de Rayon X. Rapport C.F.P. (Bordeaux), inédit.

Ferrero, J., 1966. Nouvelle méthode empirique pour le dosage des minéraux par diffraction R.X. Unpublished report C.F.P. (Bordeaux).

Ferry, S., Cotillon, P., Rio, M., 1983. Diagenèse croissante des argiles dans des niveaux isochrones de l'alternance calcaire-marne valanginienne du bassin vocontien. Zonation géographique. Comptes Rendus de l'Académie des Sciences de Paris Série II 297, 51–56.

Föllmi, K.B., Godet, A., Bodin, S., Linder, P., 2006. Interactions between environmental change and shallow-water carbonate build-up along the northern Tethyan margin and their impact on the Early Cretaceous carbon-isotope record. Paleoceanography 21, PA4211, doi:10.1029/2006PA001313.

Föllmi, K.B., Weissert, H., Bisping, M., Funk, H., 1994. Phosphogenesis, carbon-isotope stratigraphy, and carbonate-platform evolution along the Lower Cretaceous northern Tethyan margin. Geological Society of America Bulletin 106, 729–746.

Gibbs, R.J., 1977. Clay mineral segregation in the marine environment. Journal of Sedimentary Petrology 47, 237–243.

Godet, A., Blanc-Aletru, M.-C., Bodin, S., Adatte, T., Föllmi, K.B., 2005. The Hauterivian-Barremian of the Western Swiss Jura around Neuchâtel. "Colloques et Excursions" n°7. Géologie Alpine Série Spéciale, 79–96.

Godet, A., Bodin, S., Föllmi, K.B., Vermeulen, J., Gardin, S., Fiet, N., Adatte, T., Berner, Z., Stüben, D., van de Schootbrugge, B., 2006. Evolution of the marine stable carbone-isotope record during the Early Cretaceous: A focus on the late Hauterivian and Barremian in the Tethyan realm. Earth and Planetary Science Letters 242, 254–271.

Hallam, A., 1984. Continental humid and arid zones during the Jurassic and Cretaceous. Palaeogeography, Palaeoclimatology, Palaeoecology 47, 195–223.

Haq, B.U., Hardenbol, J., Vail, P.R., 1987. The chronology of fluctuating sea level since the Triassic. Science 235, 1156–1167.

Hillier, S., 1989. Clay mineral diagenesis and organic maturity indicators in Devonian lacustrine mudrock from the Orcadian Basin, Scotland. PhD thesis, University of Southampton, United Kingdom, 298 pp.

Huon, S., Burkhard, M., Hunziker, J.-C., 1994. Mineralogical, K-Ar, stable and Sr isotope systematics of K-white micas during very low-grade metamorphism of limestones (Helvetic nappes, western Switzerland). Chemical Geology (Isotope Geoscience Section) 113, 347–376.

James, N.P., 1997. The cool-water carbonate depositional realm. SEPM Special Publication N° 56. In: James, N.P., Clarke, J.A.D. (Eds.), Cool-water carbonates. Society for Sedimentary Geology, Tulsa, Oklahoma, pp. 1–20.

Klug, H.P., Alexander, L., 1974. X-ray Diffraction Procedures for Polycrystalline and Amorphous Materials. John Wiley and Sons, Inc., New York, 992 pp.

Kübler, B., 1983. Dosage quantitatif des minéraux majeurs des roches sédimentaires par diffraction X. Cahiers de l'Institut de Géologie, Université de Neuchâtel, Suisse Série AX n°1.1 and 1.2, 13 p.

Kübler, B., 1987. Cristallinité de l'illite: méthodes normalisées de préparation, méthode normalisée de mesure, méthode automatique normalisée de mesure. Cahiers de l'Institut de Géologie, Université de Neuchâtel, Suisse Série ADX n° 2.

Kübler, B., 1997. Concomitant alteration of clay minerals and organic matter during burial diagenesis. In: Paquet, H., Clauer, N. (Eds.), Soils and Sediments. Mineralogy and Geochemistry. Springer-Verlag, Berlin, pp. 327–362.

Kübler, B., Goy-Eggenberger, D., 2001. La cristallinité de l'illite revisitée: un bilan des connaissances acquises ces trente dernières années. Clay Minerals 36, 143–157.

Kübler, B., Jaboyedoff, M. (Eds.), 2000. Illite Cristallinity. Sciences de la terre et des planètes/Earth & Planetary Sciences, 331. C.R. Ac. Sc., Paris, pp. 75–89.

Lafargue, E., Marquis, F., Pillot, D., 1998. Rock-Eval 6 Applications in Hydrocarbon Exploration, Production and Soils Contamination Studies. Oil & Gas Science and Technology 53, 421–437.

Larson, R.L., Erba, E., 1999. Onset of the mid-Cretaceous greenhouse in the Barremian-Aptian: Igneous events and the biological, sedimentary and geochemical responses. Paleoceanography 14, 663–678.

Moore, D.M., Reynolds, R.C.J., 1997. X-Ray diffraction and the Identification and Analysis of Clay Minerals. Oxford University Press, New York, 378 pp.

Mutti, M., Hallock, P., 2003. Carbonate systems along nutrient and temperature gradients: some sedimentological and geochemical constraints. International Journal of Earth Sciences (Geologische Rundschau) 92, 465–475.

Persoz, F., 1982. Inventaire minéralogique, diagenèse des argiles et minéralostratigraphie des séries jurassiques et crétacées inférieures du Plateau suisse et de la bordure sud-est du Jura entre les lacs d'Annecy et de Constance. Matériaux pour la Carte Géologique de la Suisse Nouvelle Série 155, 1–52.

Ruffell, A., Mc Kinley, J., Worden, R., 2002. Comparison of clay mineral stratigraphy to other proxy palaeoclimate indicators in the Mesozoic of NW Europe. Philosophical Transactions of the Royal Society of London 360, 675–693.

Ruffell, A.H., Batten, D.J., 1990. The Barremian-Aptian arid phase in western Europe. Palaeogeography, Palaeoclimatology, Palaeoecology 80, 197–212.

Rumley, G., 1993. Sédimentologie, minéralogie et stratigraphie de l'Hauterivien dans le Jura neuchâtelois et vaudois (Suisse). PhD thesis, Université de Neuchâtel, Neuchâtel, 207 pp.

Schlanger, S.O., Jenkyns, H.C., 1976. Cretaceous oceanic anoxic events: causes and consequences. Geologie en Mijnbouw 55, 179–184.

Scholle, P.A., Arthur, M.A., 1980. Carbon Isotope Fluctuations in Cretaceous Pelagic Limestones: Potential Stratigraphic and Petroleum Exploration Tool. American Association of Petroleum Geologists Bulletin 64, 67–87.

van de Schootbrugge, B., Föllmi, K.B., Bulot, L.G., Burns, S.J., 2000. Paleoceanographic changes during the Early Cretaceous (Valanginian-Hauterivian): evidence from oxygen and carbon stable isotopes. Earth and Planetary Science Letters 181, 15–31.

van de Schootbrugge, B., 2001. Influence of paleo-environmental changes during the Hauterivian (Early Cretaceous) on carbonate deposition along the northern margin of the Tethys: Evidence from geochemical records (C, O and Sr-isotopes, P, Fe, Mn): Ph.D. thesis, Université de Neuchâtel, Neuchâtel, 291 pp.

van de Schootbrugge, B., Kuhn, O., Adatte, T., Steinmann, P., Föllmi, K., 2003. Decoupling of P- and Corg-burial following Early Cretaceous (Valanginian-Hauterivian) platform drowning along the NW Tethyan margin. Palaeogeography, Palaeoclimatology, Palaeoecology 199, 315–331.

Środoń, J., 1980. Precise identification of illite/smectite interstratification by X-Ray powder diffraction. Clays and Clay Minerals 28, 401–411.

Thiry, M., Simon-Coinçon, S., Schmitt, J.-M., 1999. Paléoaltérations kaoliniques: signification climatique et signature dans la colonne sédimentaire. Comptes

Rendus de l'Académie des Sciences de Paris. Sciences de la Terre et des Planètes 329, 853–863.
Trabold, G.L., 1996. Development of the Urgonian limestones in the Delphino Helvetic Realm (Northern Subalpine Chains, Haute-Savoie, France). Sedimentology, Sequence Stratigraphy and Biostratigraphy. PhD thesis, Université de Genève, Publications du Département de Géologie et Paléontologie 20, 1–187.
Vermeulen, J., 2002. Etude stratigraphique et paléontologique de la famille des Pulchelliidae (Ammonoidea, Ammonitina, Endomoceratacea). Géologie Alpine Mémoire H.S. N°42, 333 pp.
Weaver, C.E., 1989. Clays, Muds, and Shales. Developments in Sedimentology, 44. Elsevier Science Publishers B.V., Amsterdam, 819 pp.
Weissert, H., 1989. C-Isotope stratigraphy, a monitor of paleoenvironmental change: a case study from the Early Cretaceous. Surveys in Geophysics 10, 1–61.
Weissert, H., Lini, A., Föllmi, K.B., Kuhn, O., 1998. Correlation of Early Cretaceous carbon isotope stratigraphy and platform drowning events: a possible link? Palaeogeography, Palaeoclimatology,Palaeoecology 137, 189–203.
Wermeille, S., 1996. Etude sédimentologique, minéralogique et micropaléontologique des calcaires urgoniens de la région subalpine (Savoie, France). Coupes du Rocher de Cluses, du Borne et d'Andey: Unpublished diploma thesis, University of Neuchâtel, Neuchâtel, 129 pp.
Wissler, L., Weissert, H., Masse, J.-P., Bulot, L.G., 2002. Chemostratigraphic correlation of Barremian and lower Aptian ammonite zones and magnetic reversals. Int. J. Earth Sci.. (Geol. Rundsch.) 91, 272–279.